

## Pro-oxidant Induced DNA Damage in Human Lymphoblastoid Cells: Homeostatic Mechanisms of Genotoxic Tolerance

Anna L. Seager,<sup>\*1</sup> Ume-Kulsoom Shah,<sup>\*</sup> Jane M. Mikhail,<sup>\*</sup> Bryant C. Nelson,<sup>†</sup> Bryce J. Marquis,<sup>‡</sup>  
Shareen H. Doak,<sup>\*</sup> George E. Johnson,<sup>\*</sup> Sioned M. Griffiths,<sup>\*</sup> Paul L. Carmichael,<sup>‡</sup>  
Sharon J. Scott,<sup>‡</sup> Andrew D. Scott,<sup>‡</sup> and Gareth J. S. Jenkins<sup>\*</sup>

<sup>\*</sup>DNA Damage Research Group, Institute of Life Science, College of Medicine, Swansea University, SA2 8PP, U.K.; <sup>†</sup>National Institute of Standards and Technology (NIST), Material Measurement Laboratory-Biochemical Science Division, Gaithersburg, Maryland 20899; and <sup>‡</sup>Safety & Environmental Assurance Centre (SEAC), Unilever, Bedford, MK44 1LQ, U.K.

<sup>1</sup>To whom correspondence should be addressed at ILS, College of Medicine, Swansea University, Singleton Park, Swansea, SA2 8PP, U.K.  
Fax: +441792602147. E-mail: a.l.seager@swansea.ac.uk.

Received November 14, 2011; accepted April 17, 2012

Oxidative stress contributes to many disease etiologies including ageing, neurodegeneration, and cancer, partly through DNA damage induction (genotoxicity). Understanding the interactions of free radicals with DNA is fundamental to discern mutation risks. In genetic toxicology, regulatory authorities consider that most genotoxins exhibit a linear relationship between dose and mutagenic response. Yet, homeostatic mechanisms, including DNA repair, that allow cells to tolerate low levels of genotoxic exposure exist. Acceptance of thresholds for genotoxicity has widespread consequences in terms of understanding cancer risk and regulating human exposure to chemicals/drugs. Three pro-oxidant chemicals, hydrogen peroxide (H<sub>2</sub>O<sub>2</sub>), potassium bromate (KBrO<sub>3</sub>), and menadione, were examined for low dose-response curves in human lymphoblastoid cells. DNA repair and antioxidant capacity were assessed as possible threshold mechanisms. H<sub>2</sub>O<sub>2</sub> and KBrO<sub>3</sub>, but not menadione, exhibited thresholded responses, containing a range of nongenotoxic low doses. Levels of the DNA glycosylase 8-oxoguanine glycosylase were unchanged in response to pro-oxidant stress. DNA repair-focused gene expression arrays reported changes in *ATM* and *BRCA1*, involved in double-strand break repair, in response to low-dose pro-oxidant exposure; however, these alterations were not substantiated at the protein level. Determination of oxidatively induced DNA damage in H<sub>2</sub>O<sub>2</sub>-treated AHH-1 cells reported accumulation of thymine glycol above the genotoxic threshold. Further, the H<sub>2</sub>O<sub>2</sub> dose-response curve was shifted by modulating the antioxidant glutathione. Hence, observed pro-oxidant thresholds were due to protective capacities of base excision repair enzymes and antioxidants against DNA damage, highlighting the importance of homeostatic mechanisms in “genotoxic tolerance.”

**Key Words:** Pro-oxidants; DNA damage; reactive oxygen species; DNA repair; OGG1; antioxidants; glutathione; genotoxicology; thresholds.

Assessing the genotoxic threat of chemicals is essential in gaining a better understanding of their carcinogenic potential

to reduce any deleterious effects that may be produced through occupational and recreational exposures (Doak *et al.*, 2007; Sedelnikova *et al.*, 2010). Traditionally, regulatory authorities utilize a linear model to assess the safety of direct-acting genotoxins, whereby a mutagenic response at high doses is extrapolated to lower doses. The so-called single hit, single target hypothesis infers that there is no minimum safe exposure limit for such agents (Jenkins *et al.*, 2005). This view, however, does not account for the plethora of homeostatic mechanisms, which allow mammalian cells to tolerate low levels of genotoxins. The application of a threshold mechanism in toxicology is not new; it is widely accepted that indirect-acting genotoxins, which have non-DNA targets, may exhibit a threshold mode of action (MOA) (Elhajouji *et al.*, 2011). To date, however, the effect has been established experimentally for a limited number of DNA reactive compounds (Doak *et al.*, 2007; Jenkins *et al.*, 2005; Platel *et al.*, 2009). We recently demonstrated that genotoxic thresholds induced by the alkylating agents ethyl methane sulfonate (EMS) and methyl methane sulfonate (MMS) are due to DNA repair by the base excision repair (BER) enzyme N-methylpurine DNA glycosylase (MPG; GenBank ID:4350) and DNA repair protein O<sup>6</sup>-methylguanine-DNA methyltransferase (MGMT; GenBank ID:4255), selectively removing DNA adducts at low doses but becoming saturated (or repressed) at higher doses (Doak *et al.*, 2008; Zair *et al.*, 2011). The acceptance of dose-response thresholds for genotoxins may have substantial regulatory implications, which aid our understanding of genotoxic and neoplastic risk more fully.

An important class of DNA reactive agents present in the human environment is pro-oxidants. Mammalian cells are constantly exposed to potentially damaging reactive oxygen species (ROS) arising from multiple sources (Evans *et al.*, 2004; Loft *et al.*, 2008). Cellular defenses exist to combat attack

from ROS, including the antioxidant glutathione (GSH) and the scavenging enzyme superoxide dismutase (Forman *et al.*, 2009). Despite this, oxidative stress and damage to cellular macromolecules can arise when the number of ROS produced exceeds the antioxidant capacity of the cell. Numerous types of DNA damage can potentially arise upon exposure to ROS, with thymine bases being the most susceptible to modification and thymine glycol (TG) representing an important thymine lesion formed after treatment with oxidizing agents such as hydrogen peroxide ( $H_2O_2$ ) (Basu *et al.*, 1989).

A network of complex DNA repair pathways has evolved to avoid the perpetuation of such damage. Oxidized base lesions are repaired predominantly by the BER pathway. BER is mediated by damage-specific DNA glycosylases, with 8-oxoguanine DNA glycosylase (OGG1; GenBank ID:4968) repairing one of the most common forms of oxidatively generated DNA base damage, that is, 8-oxo-7,8-dihydroguanine (8-oxoG) (Boiteux and Radicella, 2000; Wallace, 2002). The role of repair in maintaining cellular homeostasis is highlighted by reports of BER gene activation in response to genotoxic exposure (Powell *et al.*, 2005). Further, mutation and abnormal expression of DNA repair genes, such as *ATM* (ataxia telangiectasia mutated; GenBank ID:472) and *BRCA1* (breast cancer 1, early onset; GenBank ID:672), have been directly linked with genomic instability and cancer development (Hartman and Ford, 2003; Smirnov and Cheung, 2008).

The present study focuses on DNA-pro-oxidant interaction and generates genotoxic dose responses for three pro-oxidant chemicals,  $H_2O_2$ , menadione, and potassium bromate ( $KBrO_3$ ). Two different mutagenic endpoints were assessed *in vitro* as recommended by Committee on Mutagenicity: the cytokinesis block micronucleus (CBMN) assay and *HPRT* (GenBank ID:3251) forward mutation assay, examining the induction of chromosomal damage and frequency of point mutations, respectively (Great Britain. Committee on Mutagenicity of Chemicals in Food, 2000). The principal aims were to analyze low-range dose-response curves, to establish the existence of possible genotoxic thresholds, and to explore MOA of any observed thresholds (tolerance). Compounds were chosen due to their known capacity to generate DNA damage through differential generation of various ROS.

$H_2O_2$  is a physiological constituent of living cells, continually produced by a variety of cellular pathways, and has a wide range of external applications, for instance, in bleaching and in treatment of water and sewage (Jeong *et al.*, 2010; Naik *et al.*, 2006).  $H_2O_2$  is a nonradical ROS but can react via radical-mediated routes; for example, in the presence of ferrous ions,  $H_2O_2$  undergoes Fenton's reaction to form the highly reactive hydroxyl radical ( $HO^\bullet$ ) (Pryor, 1986). Menadione is a multivitamin component and a therapeutic agent for hypothermia and cancer. In the presence of flavoenzymes, menadione may undergo reduction to a semiquinone, an extremely unstable compound that reacts rapidly with oxygen forming superoxide anion radical ( $O_2^{\bullet-}$ ) and other ROS (Chung *et al.*, 1999; Nutter

*et al.*, 1992).  $KBrO_3$  has been used as a food additive primarily in bread-making processes. European Union (EU) countries now prohibit this application due to its proven carcinogenicity. The mechanism by which  $KBrO_3$  generates damaged DNA is not fully elucidated but is believed to involve reduction of bromate by thiols such as cellular GSH to reactive intermediates including bromine radicals ( $Br^\bullet$ ) or oxides ( $BrO^\bullet$ ,  $BrO_2^\bullet$ , etc.) (Ballmaier and Epe, 1995, 2006).

## MATERIALS AND METHODS

### Chemicals

Buthionine sulfoximine (BSO),  $H_2O_2$ ,  $KBrO_3$ , menadione, and N-acetylcysteine (NAC) were all purchased from Sigma (Dorset, U.K.). All chemical dilutions were freshly prepared from stock solutions with water.

### Cell Culture

The human male near-diploid lymphoblastoid cell line AHH-1 (ATCC, Middlesex, U.K.) was cultured in RPMI 1640 (Life Technologies, Paisley, U.K.) and supplemented with 1% L-glutamine (Life Technologies) and 10% donor horse serum (BD Gentest, Oxford, U.K.) in 80-cm<sup>2</sup> flasks at 37°C, 5%  $CO_2$ . The cells were maintained at a concentration of  $1-2 \times 10^5$ /ml. AHH-1 cells were utilized in the study as they have been widely used in genetic toxicology and represent a versatile and reproducible system for examining genotoxic agents and the induction of gene locus mutation, including the analysis of damage response pathways and cellular defenses upon exposure to free radicals. AHH-1 contains native CYP1A1 activity, and despite harboring a heterozygous p53 mutation at the codon 281/282 interface within exon 8, it retains the ability to undergo DNA damage-induced apoptosis and has been reported to express phospho-p53 and p21 (Doak *et al.*, 2008; Guest and Parry, 1999). Further, previous studies on thresholds have been completed utilizing AHH-1 and have described stable background levels of chromosomal damage and point mutations (Doak *et al.*, 2007; Zair *et al.*, 2011).

### Forward Mutation Assays

We employed the *in vitro* *HPRT* assay to study induced point mutations. The assay was performed as previously described (Doak *et al.*, 2007), with the following modifications: AHH-1 cell suspensions (10 ml), at  $5 \times 10^5$ /ml, were exposed to the test chemical in 80-cm<sup>2</sup> flasks at the appropriate concentration for 24 h at 37°C, 5%  $CO_2$ . For each dose, fifteen 96-well plates for assessing mutation frequency and another five for plating efficiency were set up. Each dose was performed in triplicate.

### Micronucleus Assay

Micronuclei (MN) frequency was utilized to assess the level of chromosome aberration induction. AHH-1 (10 ml) suspensions of cells at  $1 \times 10^5$ /ml were seeded for 24 h at 37°C, 5%  $CO_2$ . Replicate flasks ( $n = 3$ , independently produced on different days) were dosed with appropriately diluted test chemical (in duplicate) for 4 h, after which cells were centrifuged, washed once in PBS, and resuspended in 10-ml fresh media containing 6- $\mu$ g/ml cytochalasin B for one cell cycle (22 h). Treated cells were harvested, resuspended in 10 ml of hypotonic solution (0.56% KCl), and centrifuged immediately. Cell suspension was resuspended in fixative 1 (methanol:acetic acid:0.9% NaCl [5:1:6 parts]) and centrifuged after a 10-min incubation period. Cells were transferred to fixative 2 (methanol:acetic acid [5:1 parts]) for a 10-min incubation, centrifuged, washed four times, and maintained in the final fixative 2 wash at 4°C for 16 h. Fixed cells were centrifuged, and 100  $\mu$ l was dropped onto polished, fixed, and hydrated slides, stained with DAPI (4',6-diamidino-2-phenylindole; 0.15  $\mu$ g/ml final concentration), and viewed under a Carl Zeiss Axio Imager fluorescence microscope. Slides were scored utilizing the Metafer 4 software version

3.5 (MetaSystems, Altusheim, Germany). An optimal scoring criterion was achieved from the development of specific classifiers adjusted to accommodate the particular lymphoblast cell line (AHH-1) and to identify binucleate cells containing MN. The criteria for identifying MN were as previously described (Fenech, 2007). A minimum of 2000 binucleated cells were scored per replicate, and each dose was performed in triplicate (an average of 6000 binucleates per dose).

#### RNA Isolation and Gene Expression Analysis

Following exposure of AHH-1 cells to the test pro-oxidants for 0, 2, 4, and 24 h time points, total cellular RNA was isolated from AHH-1 cells followed by DNase treatment using the RNeasy mini kit (Qiagen, West Sussex, U.K.) and TURBO DNA-free kit (Ambion, Huntingdon, U.K.), respectively, according to the manufacturer's instructions. Quantitative PCR of mRNA was performed as a one-step reaction, where the entire reaction from cDNA synthesis to real-time PCR amplification was performed in a single well, on a MyIQ5 cyclor optics module (Bio-Rad, Hertfordshire, U.K.). Commercially available TaqMan Gene Expression Assays and human endogenous controls were purchased from Applied Biosystems (U.K.) and supplied as premixed primers and FAM/MGB probe. To perform one-step real-time PCR, *OGG1* target gene (Hs00213454\_m1\*) and *HPRT* reference gene (4333768) probes were used in conjunction with QuantiFast Probe RT-PCR kit (Qiagen). Approximately 0.2 µg RNA was used for cDNA synthesis and PCR in a reaction volume of 20 µl, containing 10 µl of 2× QuantiFast Probe RT-PCR Master Mix, 0.4 µl QuantiFast RT Mix, and 1 µl of TaqMan probe mix (primers and probe at final concentrations of 900nM and 250nM, respectively). The following PCR reaction protocol was used: initially cDNA production occurred for one cycle at 50°C for 10 min followed by 95°C for 5 min. Subsequently, PCR was initiated for 40 cycles of 95°C for 10 s and 61°C for 30 s. Reactions were performed in triplicate, and the level of gene expression was reported as the ratio between the mRNA level of the target gene and the *HPRT* reference gene using the relative standard curve method.

#### Western Blot Analysis

Following exposure to the test pro-oxidants for 0-, 2-, 4-, and 24-h time points, total cellular protein was isolated from AHH-1 cells. Cells were pelleted by centrifugation, washed in ice-cold PBS, and then lysed in RIPA buffer (Sigma), supplemented with protease inhibitor cocktail (Sigma) at 4°C for 5 min. Cells were further lysed by agitation and centrifugation, and the cell pellet was discarded. Protein extracts (30 ng) of AHH1 cells were resolved on 10% SDS-PAGE at 120 V, transferred onto polyvinylidene difluoride membranes (Bio-Rad), and blocked for 1 h at room temperature with 5% bovine serum albumin in TBS-T (20mM Tris [pH 7.6], 125mM NaCl, 0.1% (v/v) Tween20). Membranes were incubated with monoclonal mouse anti-OGG1 (Sigma), polyclonal rabbit anti-beta tubulin (AbCam, Cambridge, U.K.), monoclonal rabbit anti-ATM (Cell Signaling Technology, MA), polyclonal rabbit anti-*BRCA1* (Cell Signaling Technology), or monoclonal rabbit anti-beta actin (Cell Signaling Technology) antibodies overnight at 4°C. Following washing (4 × 5 min in TBS-T), membranes were incubated with appropriate horseradish peroxidase conjugated secondary antibodies (AbCam). Protein bands were detected using the Immun-Star WesternC chemiluminescence kit (Bio-Rad). Membranes were visualized using the Bio-Rad Chemidoc XRS, and average band density analysis was performed using Quantity One version 4.6.3 (Bio-Rad).

#### Human DNA Repair PCR Arrays

To assess the role of a wider range of DNA repair enzymes in the observed nonlinear damage responses to pro-oxidants, gene expression PCR arrays tailored for DNA repair were utilized. AHH-1 cells were treated with specific doses above and below confirmed threshold inflection points (IPs), which were 5µM and 25µM H<sub>2</sub>O<sub>2</sub>, 0.2mM and 0.8mM KBrO<sub>3</sub>, and 0.5mM and 3.5mM menadione, for 4 h, and the RNA was extracted. RNA (1.6 µg) from each sample was reverse transcribed into cDNA using the RT<sup>2</sup> First Strand Kit (Qiagen). Gene expression was performed utilizing Human DNA Repair RT<sup>2</sup> Profiler PCR Arrays (PAHS-042A) and 2× SABiosciences RT<sup>2</sup> qPCR Master Mix

(Qiagen) and MyiQ real-time PCR Platform (Bio-Rad) according to the manufacturer's instructions. Gene expression was normalized using five housekeeping genes within the array and quantified using the Ct method by accessing the PCR Array Data Analysis Web Portal (<http://pcrdataanalysis.sabiosciences.com/pcr/arrayanalysis.php>).

#### Gas Chromatography/Mass Spectrometry Determination of Oxidatively Induced DNA Damage

Gas chromatography/mass spectrometry (GC/MS) with isotope dilution was used to determine the absolute levels of five different oxidatively modified bases: 8-oxoG, TG, 5-hydroxy-5-methylhydantoin (5-OH-5-MeHyd), 2,6-diamino-4-hydroxy-5-formamidopyrimidine (FAPyG), and 4,6-diamino-5-formamidopyrimidine (FAPyA). AHH-1 cells were seeded for 24 h and treated with 0, 5, and 25µM/ml H<sub>2</sub>O<sub>2</sub> for 4 h. Following washing, DNA was extracted from the treated cells using the DNeasy Blood & Tissue Kit (Qiagen). The DNA was precipitated, and GC/MS analyses were performed as previously described (Dizdaroglu, 1985; Jaruga *et al.*, 2008).

#### Alteration of Cellular GSH Levels

In order to modulate GSH levels prior to measuring pro-oxidant-induced MN, GSH was either supplemented or depleted. AHH-1 (10 ml) suspensions of cells at  $1 \times 10^5$ /ml were seeded for 24 h at 37°C, 5% CO<sub>2</sub>. Cells were dosed with 2mM NAC to promote GSH levels and increase cellular antioxidant status or with 0.5mM BSO, an inhibitor of GSH synthesis, for 24 h prior to pro-oxidant treatment and CBMN assay (as previously described). The levels of GSH in treated cells were estimated utilizing the Glutathione Assay kit (Sigma) according to the manufacturer's instructions.

#### Statistical Analysis

For the genotoxicity data and DNA adduct data, a one-way ANOVA, followed by a Dunnett's *post hoc* test, was used to determine if any of the treatment doses were significantly different from the zero dose, except when cells were pretreated with BSO or NAC, where a *t*-test was employed. The hockey stick modeling of apparent thresholds was carried out using software, kindly provided by Lutz and Lutz (2009) and implemented in the R package. A *t*-test was performed to establish any differences between relative protein and mRNA expression of *OGG1* after pro-oxidant treatments at different time points analyzed. Independent sample *t*-test was utilized to analyze differences in normalized protein levels of *ATM* and *BRCA1* after treatment with H<sub>2</sub>O<sub>2</sub> (0–25µM) or KBrO<sub>3</sub> (0–0.8mM).

## RESULTS

The CBMN and *HPRT* forward mutation assays were used to assess the induction of chromosomal aberration (MN formation) and frequency of point mutations, respectively, after exposure of AHH-1 lymphoblastoid cells to low concentrations of the oxidizing agents. The range of concentrations used was determined following initial dose-setting experiments, analyzing genotoxicity and assessing cytotoxicity utilizing relative population doubling calculations in satellite cultures (data not shown). To ensure that any observed genetic damage was not due to cytotoxicity-related mechanisms, only those concentrations leading to more than 50% cell viability were analyzed (data not shown). Investigations into the MOA behind these threshold responses involved analysis of levels of DNA repair enzymes involved in the repair of oxidative damage, assessment of the levels of oxidatively modified bases

in exposed DNA, and analysis of the effect of antioxidant status on the dose-response curves to chromosome damage. To ensure that cellular exposure to ROS was occurring at low doses of pro-oxidants, oxidation of the nonfluorescent probe 2',7'-dichlorofluorescein-diacetate (DCFH-DA) to the fluorochrome 2,7-dichlorofluorescein (DCF) was used as an index to quantify the overall level of intracellular ROS produced by 0–100 $\mu$ M H<sub>2</sub>O<sub>2</sub> (Supplementary fig. S1).

#### Gene Mutation Induction

The *HPRT* forward mutation assay was used here to investigate the mutagenic activity of H<sub>2</sub>O<sub>2</sub>, KBrO<sub>3</sub>, and menadione. All three pro-oxidants demonstrated a range of low doses with minimal levels of mutation induction in AHH-1 human lymphoblastoid cells, compared with solvent control data (Fig. 1). The first statistically significant increase in mutation frequency above background levels (lowest observed effect level [LOEL]) was 18 $\mu$ M for H<sub>2</sub>O<sub>2</sub> ( $p = 0.004$ ), 0.5mM for KBrO<sub>3</sub> ( $p = 0.004$ ), and 2.9 $\mu$ M for menadione ( $p = 0.001$ ) utilizing one-way ANOVA, followed by a Dunnett's *post hoc* test. Further analysis of these results applying a "hockey-stick model" developed by Lutz and Lutz (2009) rejected linearity of each dose-response curve while supporting a threshold model ( $p < 0.05$ ) and showed that H<sub>2</sub>O<sub>2</sub> had an IP (or threshold dose) at 7.3 $\mu$ M with lower confidence interval (CI) of 2.04 $\mu$ M; KBrO<sub>3</sub>, an IP of 0.18mM with lower CI of 0.08mM; and menadione, an IP of 1.89 $\mu$ M with lower CI of 0.76mM (Fig. 1) (Lutz and Lutz, 2009).

#### Chromosomal Damage Induction

The dose-response relationships, with respect to the induction of chromosome aberrations, obtained after pro-oxidant treatments with H<sub>2</sub>O<sub>2</sub>, KBrO<sub>3</sub>, and menadione are illustrated in Figure 2. LOEL concentrations of 25 $\mu$ M ( $p = 0.03$ ), 0.6mM ( $p = 0.007$ ), and 2.9 $\mu$ M ( $p = 0.036$ ) were identified for exogenous treatment with H<sub>2</sub>O<sub>2</sub>, KBrO<sub>3</sub>, and menadione, respectively. Subsequent increases in concentration above each LOEL produced a progressive rise in cellular DNA damage, as detected by a higher incidence of MN. Hockey-stick statistical modeling of the data using the Lutz approach rejected a linear fit to the dose-response curves and confirmed an IP (threshold value) of 10.88 $\mu$ M with lower CI of 5.93 $\mu$ M and 0.35mM with lower CI of 0.22mM, for H<sub>2</sub>O<sub>2</sub> and KBrO<sub>3</sub>, respectively. The dose-response curve for menadione, despite indicating a nonlinear response for the induction of genotoxic damage, favored a linear model and did not achieve significance when hockey-stick modeling was performed on the data.

#### BER Glycosylase Cellular Levels

In order to examine the protective mechanisms behind the genotoxic tolerance to low doses of pro-oxidants shown here, we focused firstly on the role of DNA repair. Previous work on thresholded responses for the alkylating agents has demonstrated upregulation of the DNA repair enzymes *MPG* and *MGMT*

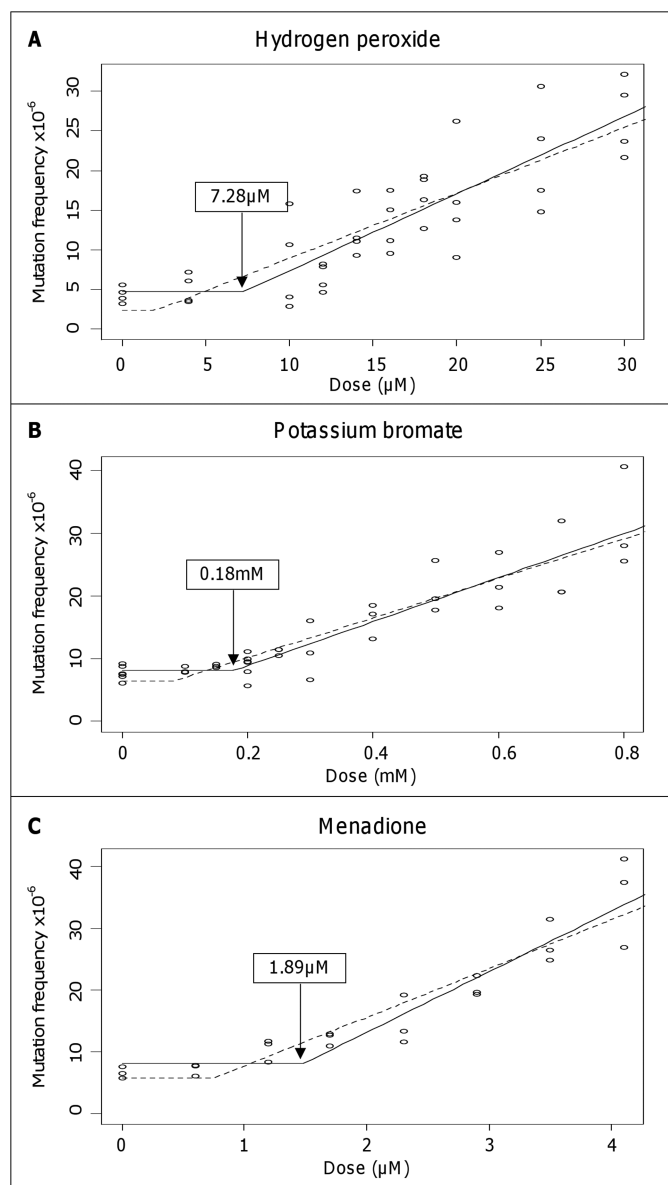


**FIG. 1.** Gene mutation frequency in response to pro-oxidants. Dose-response relationships of hydrogen peroxide (H<sub>2</sub>O<sub>2</sub>), potassium bromate (KBrO<sub>3</sub>), and menadione in the AHH-1 cell line with respect to *HPRT* gene mutation frequency. Hockey-stick statistical modeling analysis has been applied to each data set to calculate the IP, probability for nonlinearity ( $p$ ), and  $Y$ -intercept. (A) H<sub>2</sub>O<sub>2</sub>, threshold, IP = 7.28 $\mu$ M, lower IP/CI = 2.04 $\mu$ M,  $Y = 1.95$ , and  $p = 0.038$ . (B) KBrO<sub>3</sub>, threshold, IP = 0.18mM, lower IP/CI = 0.08mM,  $Y = 6.11$ , and  $p = 0.004$ . (C) Menadione, threshold, IP = 1.89 $\mu$ M, lower IP/CI = 0.76 $\mu$ M,  $Y = 5.05$ , and  $p = 0.004$ .

by EMS and MMS, respectively, at doses below the threshold (Doak *et al.*, 2008; Zair *et al.*, 2011). Because 8-oxoG is a major DNA lesion formed as a consequence of ROS exposure and 8-oxoG in DNA is primarily repaired by the DNA glycosylase *OGG1*, the mRNA and protein levels of this enzyme were measured in response to specific pro-oxidant treatment (in this case, H<sub>2</sub>O<sub>2</sub>). *OGG1* expression levels in treated and untreated

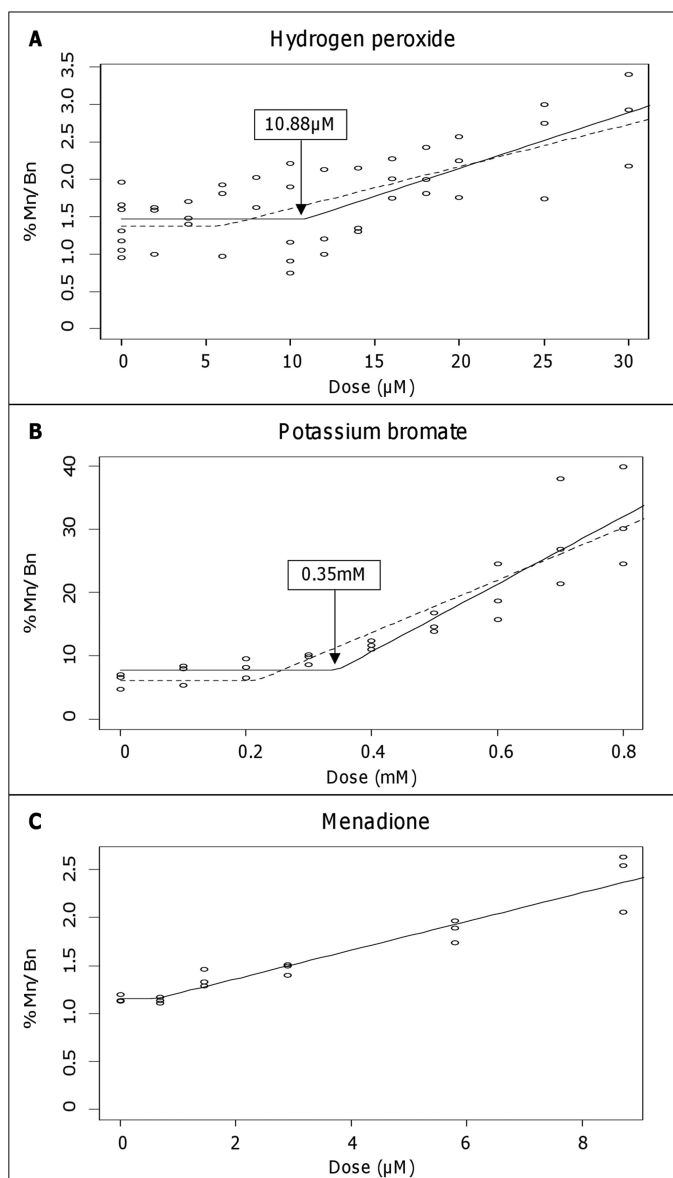


**FIG. 2.** Chromosomal damage in response to pro-oxidants. Dose-response relationships of hydrogen peroxide ( $\text{H}_2\text{O}_2$ ), potassium bromate ( $\text{KBrO}_3$ ), and menadione in the AHH-1 cell line with respect to micronucleus frequency. Hockey-stick statistical modeling analysis has been applied to each data set to calculate the IP, probability for nonlinearity ( $p$ ), and  $Y$ -intercept. (A)  $\text{H}_2\text{O}_2$ , threshold, IP = 10.88 $\mu\text{M}$ , lower IP/CI = 5.93 $\mu\text{M}$ ,  $Y$  = 1.32, and  $p$  = 0.023. (B)  $\text{KBrO}_3$ , threshold, IP = 0.35mM, lower IP/CI = 0.22mM,  $Y$  = 1.05, and  $p$  = 0.002. (C) Menadione, linear, and  $p$  = 0.35. *Mn/Bn* %: Percentage of binucleated cells containing one or more MN.

AHH-1 lymphoblastoid cells, measured by real-time RT-PCR, are represented in Figure 3A. No significant modulation in *OGG1* expression in response to  $\text{H}_2\text{O}_2$  treatment (0–50 $\mu\text{M}$ ) was observed at any of the time points (0–24 h) studied. *OGG1* protein levels in AHH-1 cells following oxidative insult were also analyzed by Western blotting and normalized to beta-tubulin expression (Fig. 3B). Similar to mRNA levels, treatment with

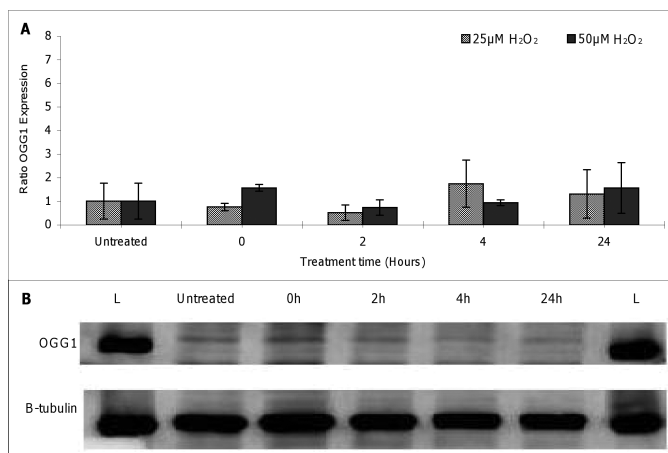


**FIG. 3.** Effect of hydrogen peroxide on *OGG1* levels. (A) Effect of hydrogen peroxide ( $\text{H}_2\text{O}_2$ ) on *OGG1* expression in AHH-1 cells. Cells were treated with 0–50 $\mu\text{M}$  of  $\text{H}_2\text{O}_2$ , and total RNA was extracted between 0 and 24 h. Levels of *OGG1* mRNA were assessed by real-time RT-PCR. Values were normalized to levels of the constitutively expressed housekeeping gene, *HPRT*, and represent the mean (SD) fold change from control levels at each time point. Each data point represents three independent measurements. (B) Western blot of *OGG1* protein and loading control B-tubulin in AHH-1 cells following treatment with 25 $\mu\text{M}$   $\text{H}_2\text{O}_2$  for 0, 2, 4, and 24 h; L: Ladder.

$\text{H}_2\text{O}_2$  (0–50 $\mu\text{M}$ ) had no detectable effect on the amount of *OGG1* protein recovered from nuclear extracts at any of the treatment periods (0–24 h) monitored; comparable results were observed for treatment with 1mM  $\text{KBrO}_3$  (results not shown).

#### Human DNA Repair PCR Arrays

To investigate the effects of pro-oxidant treatment on a wider range of DNA repair genes within this interesting thresholded region, treated cells were analyzed using DNA repair-directed PCR gene expression arrays. Because only  $\text{H}_2\text{O}_2$  and  $\text{KBrO}_3$  showed thresholds for both point mutation and chromosome damage, these studies concentrated on these two pro-oxidants. The PCR expression arrays focus on a selected panel of 84 genes involved in the base excision, nucleotide excision, mismatch, double-strand break, and other DNA repair processes (Supplementary fig. S2). Numerous fold changes in expression, compared with untreated control cells, were observed above and below the threshold doses (Table 1). *ATM*, for example (an important gene involved in the signaling response to DNA damage), showed unchanged expression levels at concentrations below the threshold doses but was observed to be 2.13-fold ( $\text{H}_2\text{O}_2$ ) and 4.0-fold ( $\text{KBrO}_3$ ) downregulated above the threshold dose for chromosome damage induction, suggestive of a relatively higher degree of damage recognition below the threshold. The cancer susceptibility gene *BRCA1*, involved in the repair of DNA double-strand breaks (DSBs), was upregulated by 2.39- and 2.04-fold ( $\text{H}_2\text{O}_2$  and  $\text{KBrO}_3$ , respectively) at concentrations below but not above the thresholds for chromosomal damage in both chemicals.  $\text{H}_2\text{O}_2$ -treated cells also exhibited a

**TABLE 1**  
**Alterations in DNA Repair Gene Expression Above and Below**  
**the Threshold for Chromosome Damage Induction**

| Gene symbol | Fold change in gene expression          |  |                         |                         |
|-------------|---|--|-------------------------|-------------------------|
|             | 5 $\mu$ M H <sub>2</sub> O <sub>2</sub> | 25 $\mu$ M H <sub>2</sub> O <sub>2</sub> | 0.2mM KBrO <sub>3</sub> | 0.8mM KBrO <sub>3</sub> |
| APEX1       | 2.69                                    | 1.14                                     | n/a                     | 2.57                    |
| ATM         | 0.52                                    | -0.47                                    | 1.08                    | -0.25                   |
| BRCA1       | 2.39                                    | 1.71                                     | 2.04                    | 1.89                    |
| ERCC4       | 0.55                                    | 0.74                                     | 0.66                    | -0.5                    |
| FEN1        | -0.46                                   | 0.83                                     | 0.61                    | -0.44                   |
| LIG3        | 0.53                                    | 0.7                                      | 0.62                    | -0.47                   |
| MUTYH       | 0.54                                    | 0.74                                     | 0.62                    | -0.46                   |
| PNKP        | -0.41                                   | 0.71                                     | 0.53                    | -0.34                   |
| TOP3B       | 0.51                                    | 0.79                                     | 0.55                    | -0.43                   |

Note. n/a, not applicable.

2.69-fold increase in expression of *APEX1* (APEX nuclease [multifunctional DNA repair enzyme] 1; GenBank ID:328) at a concentration below, but not above, the threshold dose, indicative of a role for BER in minimizing chromosome damage at low H<sub>2</sub>O<sub>2</sub> doses. Further, the BER DNA glycosylase *MUTYH* (mutY homolog [*Escherichia coli*]; GenBank ID:4595), which catalyzes the removal of adenine bases from the DNA backbone at sites where adenine is inappropriately paired with guanine, cytosine, or 8-oxoG, was downregulated by 2.17-fold after exposure to 0.8mM KBrO<sub>3</sub>.

#### Relative Levels of DNA Damage Response Proteins

To further investigate the gene expression changes observed during the PCR gene array experiments and to ascertain whether such expression changes were consistently observed at the protein level, the amount of *ATM* and *BRCA1* protein recovered from nuclear extracts after pro-oxidant treatment was determined in AHH-1 cells. Cells were dosed with H<sub>2</sub>O<sub>2</sub> and KBrO<sub>3</sub> at concentrations above and below the thresholds for chromosome damage induction, and relative protein levels were deduced by Western blotting via the examination of band intensities of *ATM* or *BRCA1* normalized to beta-actin loading controls (Fig. 4). Unlike the alterations in *ATM* and *BRCA1* mRNA expression observed following treatment with concentrations of H<sub>2</sub>O<sub>2</sub> above (25 $\mu$ M) or below (5 $\mu$ M) the threshold, no significant threshold-dependent differences in the levels of these DNA repair proteins were detected (Fig. 4A). Treatment with 0.2mM KBrO<sub>3</sub> (below the threshold) appeared to induce an increase in protein levels of both *ATM* and *BRCA1* (Fig. 4B), which then decreased at 0.8mM KBrO<sub>3</sub> (above the threshold) to levels comparable to untreated samples; however, these differences were not deemed significant by independent sample *t*-test.

#### GC/MS Determination of Oxidatively Induced DNA Damage

Four out of the five modified bases were detected in the AHH-1 DNA extracts (Fig. 5). The FAPyA lesion was not detectable in either the control or the H<sub>2</sub>O<sub>2</sub>-treated samples, most likely

due to the low amount (~30  $\mu$ g) of extracted DNA/sample available for MS analysis. Of the four detected lesions, the levels of the 8-oxoG, FAPyG, and 5-OH-5-MeHyd lesions in the H<sub>2</sub>O<sub>2</sub>-treated samples were not significantly different from the background levels in the control samples. The TG lesion, however, was found to be significantly ( $p = 0.0259$ ) increased in the 25 $\mu$ M H<sub>2</sub>O<sub>2</sub>-treated sample (Fig. 5D), in comparison with the TG background level in the control samples. The level of TG in the 5 $\mu$ M H<sub>2</sub>O<sub>2</sub>-treated sample was not significantly different from the TG levels in the controls. The accumulation of TG in the 25 $\mu$ M H<sub>2</sub>O<sub>2</sub>-treated sample could potentially have biological relevance as TG is a cytotoxic lesion that is a known block to DNA polymerase.

#### Impact of GSH on Pro-oxidant-Induced DNA Damage

GSH is the principal nonprotein thiol involved in the antioxidant cellular defense, playing a critical role in protecting cells from oxidative damage and the toxicity of xenobiotic electrophiles, as well as maintaining redox homeostasis (Forman *et al.*, 2009). To elucidate the function of antioxidants in the observed genotoxic threshold effects described above, intracellular levels of GSH were modified, and the shapes of the resultant dose-response curves for H<sub>2</sub>O<sub>2</sub>, with respect to chromosomal damage, were assessed. AHH-1 cells were pretreated with BSO (0.5mM), a specific GSH synthesis inhibitor, or NAC (2.0mM), a GSH precursor, for 24 h, and the effects on H<sub>2</sub>O<sub>2</sub>-induced DNA damage were determined by the CBMN assay (Fig. 6). BSO pretreatment altered the shape of the H<sub>2</sub>O<sub>2</sub> dose-response curve significantly from a thresholded curve to a linear dose-response, which saturates at higher doses. BSO pretreatment reduced the first dose to induce a statistically significant increase in genetic damage from 18 $\mu$ M to 8 $\mu$ M ( $p = 0.0008$ ), which indicates that GSH depletion by BSO (confirmed utilizing a GSH assay) reduces protection against oxidatively induced DNA damage, at low-dose treatments. Furthermore, statistically significant increases in MN frequency were observed in BSO pretreated cells at 10 $\mu$ M ( $p < 0.001$ ) and 12 $\mu$ M ( $p < 0.01$ ) H<sub>2</sub>O<sub>2</sub> compared with cells without pretreatment. In contrast, NAC pretreated cells had significantly lower levels of MN induction at 18 $\mu$ M ( $p < 0.001$ ) and 25 $\mu$ M ( $p < 0.01$ ) H<sub>2</sub>O<sub>2</sub> compared with H<sub>2</sub>O<sub>2</sub> cells without pretreatment, suggestive of a protective effect of enhanced GSH status.

#### DISCUSSION

Elevated cellular levels of ROS can imbalance homeostasis and create oxidative stress, and chronic exposure to this stress can cause permanent genomic changes. Accumulation of oxidative lesions has been associated with ageing and a host of human diseases including cancer, chronic inflammation, atherosclerosis, and neurodegenerative diseases such as Alzheimer's disease (Sedelnikova *et al.*, 2010). The use of oxidative DNA damage measurements in populations may

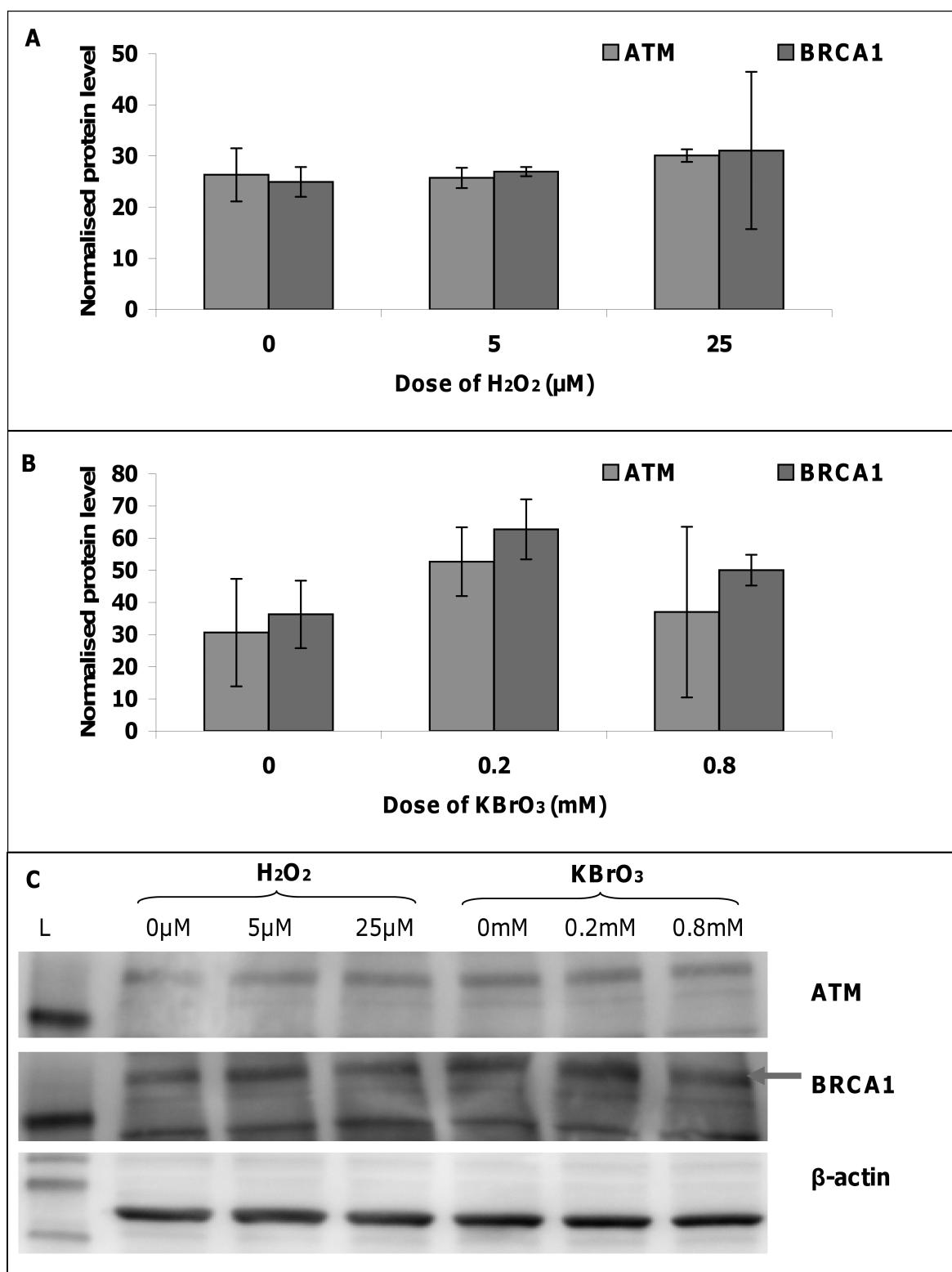


**FIG. 4.** Effects of pro-oxidants on protein levels of *ATM* and *BRCA1*. (A) Effect of hydrogen peroxide (H<sub>2</sub>O<sub>2</sub>) on *ATM* and *BRCA1* protein levels recovered from AHH-1 cells treated for 4 h with concentrations above (25μM) and below (5μM) the genotoxic threshold for DNA damage induction. (B) Effect of potassium bromate (KBrO<sub>3</sub>) on *ATM* and *BRCA1* protein levels recovered from AHH-1 cells treated for 4 h with concentrations above (0.2mM) and below (0.8mM) the genotoxic threshold for DNA damage induction. *Normalized protein level*: Relative protein concentration calculated using membrane band intensities normalized to beta-actin loading control band intensities. *Bars*: Standard deviation.

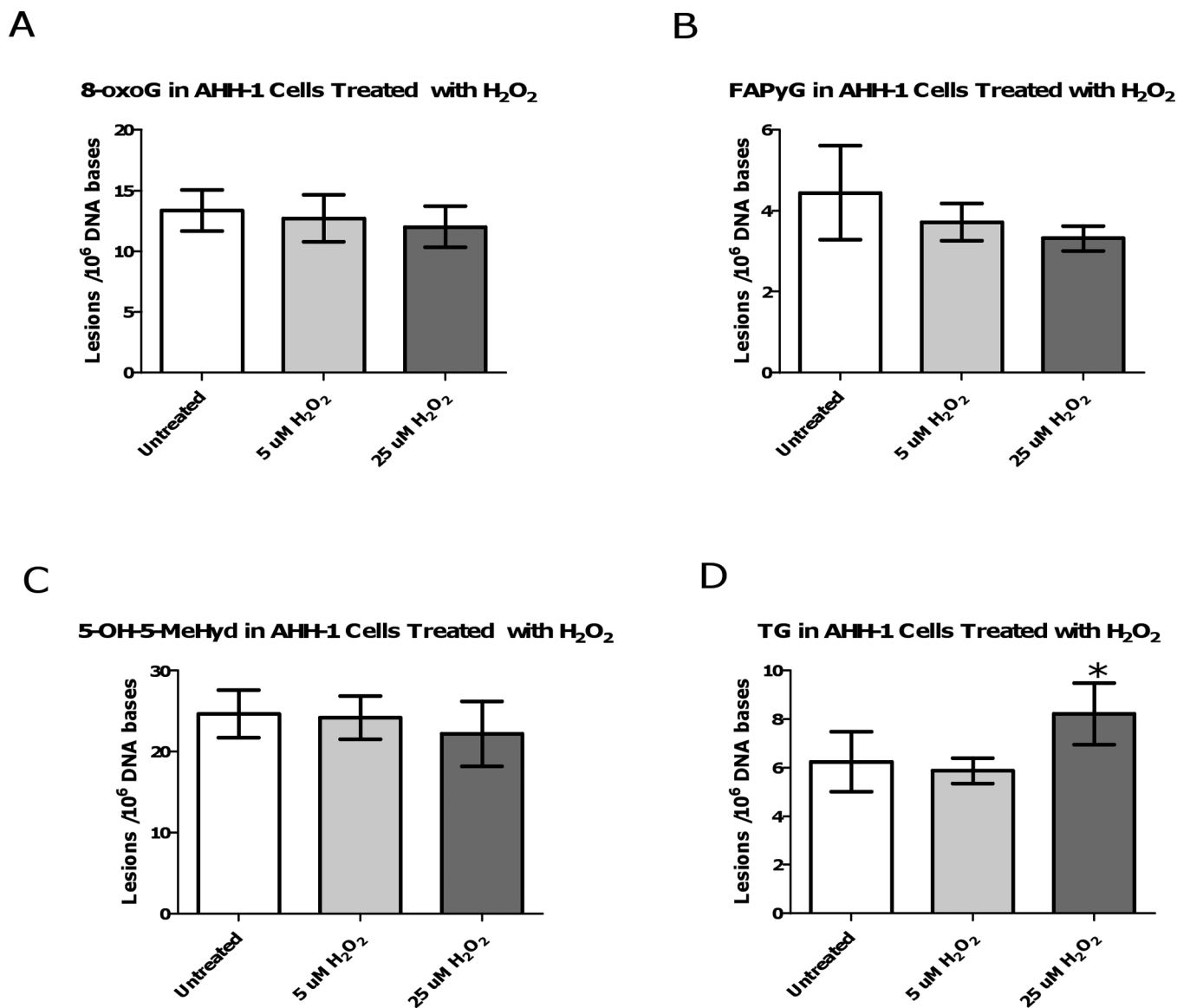


**FIG. 5.** Determination of oxidatively induced DNA damage in hydrogen peroxide-treated AHH-1 cells. (A) Accumulation of 8-oxoG in relation to exposure dose, (B) accumulation of FAPyG in relation to exposure dose, (C) accumulation of 5-OH-5-MeHyd in relation to exposure dose, and (D) accumulation of TG in relation to exposure dose. \*Indicates statistically significant result ( $p < 0.05$ ) compared with that of the control samples using one-way ANOVA followed by Dunnett's multiple comparison test. All data points represent the mean of 4 independent measurements. Uncertainties are standard deviations.

have important implications for human health risk assessment, distinguish relevant environmental exposures, and predict the frequency of disease (Hatt *et al.*, 2008; Loft *et al.*, 2008).

Traditionally, characterization of DNA-reactive agents has involved the assumption of a linear relationship between genotoxin exposure and induction of mutagenic modifications (Henderson *et al.*, 2000). This view, however, does not account for homeostatic mechanisms that potentially counteract DNA damage induced after genotoxic exposure. Knowledge of the dose-response relationship of a given chemical is paramount; if a threshold exists, safe levels can be calculated; if there is a linear dose-response, there are no safe exposure levels. This

can have economic implications, impacting the availability and use of certain compounds.

To investigate the biological significance of low-dose exposures, a robust analysis of mutation and chromosomal damage induction was performed with the DNA-reactive compounds H<sub>2</sub>O<sub>2</sub>, KBrO<sub>3</sub>, and menadione. All three pro-oxidants displayed a range of low doses with no statistically significant increase above background levels of DNA damage induction. Objective analysis of the data employing hockey stick statistical modeling demonstrated inflection (threshold) points for each of the dose relationships, except for chromosomal damage induction in menadione, which conformed to a linear model.

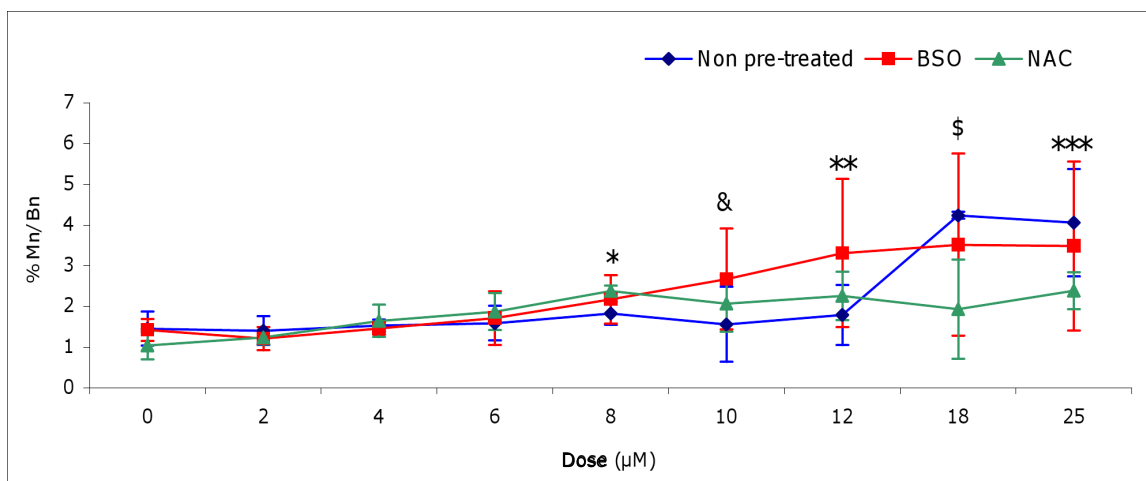


**FIG. 6.** Pro-oxidant dose response following alteration of cellular GSH antioxidant levels. Effect of BSO (0.5mM) or NAC (2.0mM) pretreatment on the frequency of hydrogen peroxide ( $H_2O_2$ )-induced MN in AHH-1 cells. \*At  $8\mu M H_2O_2$ , first significant increase in MN frequency above the control in BSO pretreated cells ( $p = 0.0008$ ) as determined by  $t$ -test. &: At  $10\mu M H_2O_2$ , BSO pretreated cells demonstrated a statistically significant increase in percentage MN compared with non-pretreated and NAC pretreated cells ( $p < 0.001$  and  $p < 0.05$ , respectively); \*\*At  $12\mu M H_2O_2$ , BSO pretreated cells showed a statistically significant elevation in MN compared with non-pretreated cells ( $p < 0.01$ ); \$: At  $18\mu M H_2O_2$ , first statistically significant increase in MN frequency above the control in non-pretreated cells ( $p < 0.0001$ ); also, non-pretreated cells exhibited statistically significant higher levels of MN to NAC pretreated cells ( $p < 0.001$ ); \*\*\*At  $25\mu M H_2O_2$ , non-pretreated cells had statistically significant higher levels of MN than NAC pretreated cells ( $p < 0.01$ ). Mn/Bn%: Percentage of binucleated cells containing one or more MN.

Menadione may thus be considered a nonthresholded compound overall. The linear relationship of damage induction observed after menadione exposure may be explained by the reported production of a high frequency of DNA strand scission by the compound mediated by  $HO^\bullet$ , which may be too extensive for the repair machinery to correct, even at low doses (Nutter *et al.*, 1992). Although DNA strand breaks occur after exposure to  $H_2O_2$  and  $KBrO_3$ , other oxidative lesions such as 8-oxoG and TG occur preferentially (Cadet *et al.*, 2010; Kawanishi and Murata, 2006).

Thresholds were reported at lower concentrations (1.5- to 2-fold) for point mutations than for MN induction, which may be explained by the higher probability of a single oxidative lesion formation yielding a base substitution, compared with a DSB arising from multiple clustered lesions. Indeed, abortive BER processing of radical damage can form DSBs when the position of lesions is closely opposed on the two strands (Wallace, 2002).

Several mechanisms may be responsible for contributing to genotoxic thresholds in response to ROS; however, DNA repair is likely to be the primary mode of defense. Repair pathways may well successfully remove newly formed adducts at low doses, and if the rate of lesion repair is faster than its rate of formation, a no observed-effect limit (NOEL) will result. We have previously noted that thresholds for alkylating agents (EMS and MMS) are accompanied by increases in the expression of DNA repair genes *MGMT* and *MPG* (Doak *et al.*, 2008; Zair *et al.*, 2011).

A well-studied biomarker of oxidative damage, and a key repairable DNA lesion induced by the pro-oxidants studied,

is 8-oxoG. 8-oxoG is a premutagenic DNA lesion due to its propensity to mispair with adenine, generate errors in replication, and G:C to T:A transversions. It is a substrate for the BER pathway, initiated by the *OGG1* enzyme (Boiteux and Radicella, 2000; Nishimura, 2002). To investigate the potential of *OGG1* as a thresholded MOA, gene and protein expression of *OGG1* was examined. No modulation in *OGG1* levels was observed in response to oxidative stress, which is in agreement with other studies (Mistry and Herbert, 2003; Saitoh *et al.*, 2001). Furthermore, *OGG1* has been described as a housekeeping gene with a constant level of expression throughout the cell cycle (Dhenaut *et al.*, 2000). Basal, not inducible, expression of *OGG1*, therefore, may play a role in the maintenance of homeostasis in the presence of low levels of pro-oxidants.

A lack of *OGG1* induction may reflect the redundancy that exists between BER glycosylases and indeed between other pathways to repair oxidative lesions. Further investigation into the responses of other DNA repair genes to pro-oxidant stress was needed, and to fulfill this requirement, the gene expression profile of 84 key DNA repair enzymes was compared at doses above and below the thresholds of chromosome damage induction observed for  $H_2O_2$  and  $KBrO_3$  (S2). For most of the nine genes with altered expression, there was no clear pattern for the two chemicals, and therefore, it is difficult to propose a direct mechanistic link in which a threshold level of exposure determines a switch in the expression of the DNA damage response program. Despite this, two repair genes showed interesting results: *ATM*, a central component of the DSB repair pathway in mammalian cells, was downregulated above

the threshold doses for damage induction and *BRCA1*, a nuclear phosphoprotein that plays a role in maintaining genomic stability, was upregulated below the threshold doses for damage induction in both  $H_2O_2$  and  $KBrO_3$ .

Analysis of protein levels of these DNA damage response genes following exposure to pro-oxidants, however, did not substantiate the PCR array findings, and no significant alterations in the protein levels of *ATM* or *BRCA1* were observed above or below the genotoxic thresholds. Thus, although DSB may occur under oxidative stress conditions, such as when ROS-induced DNA damage interferes with either DNA replication or transcription, for example, during the processing of bulky DNA adducts such as FAPyG produced from ring opening of guanine upon exposure to  $HO^\bullet$ ; it is not involved in the MOA of genotoxic thresholds observed for pro-oxidants. In agreement with this conclusion, in this study, FAPyG lesions were observed at similar levels at doses above and below the  $H_2O_2$  threshold and thus appeared to be repaired effectively or were not formed upon exposure to low doses. In contrast, TG levels were significantly higher in 25  $\mu M$ , but not in 5  $\mu M$ ,  $H_2O_2$ -treated samples than in untreated controls.

TG is the most common thymine lesion found after treatment with oxidizing agents and exerts significant distortion on the duplex DNA molecule, blocking replication. However, there are instances whereby DNA polymerases can by-pass TG and a low level of misincorporation of guanine opposite TG occurs, giving rise to mutation (Wallace, 2002). The presence of higher levels of TG above the threshold suggests a role for this lesion and BER in the observed genotoxic thresholds. The BER glycosylases NEIL1 (nei endonuclease VIII-like 1; GenBank ID:79661) and NTHL1 (*nth* endonuclease III-like 1; GenBank ID: 4913) may successfully remove TG at low doses, but above the threshold the glycosylases are "saturated"; lesions start to escape repair, becoming fixed permanent defects, and subsequent increases in dose result in a more linear increase in damage. Alternatively, formation of TG may be reduced below the threshold due to lower exposure to ROS.

DNA repair represents but one tier of protection against oxidatively generated DNA damage present in multicellular organisms. Antioxidants may also contribute to the above described thresholds. Alteration of the antioxidant status of cells via the manipulation of GSH levels transformed the shape of the dose-response curve of  $H_2O_2$ -induced chromosomal damage. For example, inhibition of GSH by BSO altered the shape of the curve from a nonlinear threshold to a more linear response and reduced the lowest dose to induce a statistically significant increase in genetic damage from 25  $\mu M$  to 8  $\mu M$   $H_2O_2$ . Furthermore, boosting GSH levels with NAC shifted the dose response to the right, with treated cells showing significantly lower levels of MN induction at 18  $\mu M$  and 25  $\mu M$   $H_2O_2$  compared with  $H_2O_2$  cells without pretreatment. Such effects suggest a causal role for GSH in the genotoxic thresholds of pro-oxidants, competing with DNA to accept electrons from ROS, removing their oxidative capacity and the potential to create mutagenic

lesions. Altering the redox status *in vitro* by increasing the levels of antioxidants has beneficial, protective effects against pro-oxidant agents.

Although it is difficult to extrapolate from the *in vitro* data described here to an *in vivo* setting, the existence of a NOEL implies at least a pragmatic threshold for carcinogenicity of  $H_2O_2$  and  $KBrO_3$ . Genotoxic tolerance to low levels of pro-oxidant chemicals appears to be due, in part, to basal BER DNA repair plus the protective capacity of antioxidants against DNA damage. The abundance of repair pathways and significant redundancy achieved by overlapping substrates in maintaining REDOX homeostasis suggest that the persistence of oxidative DNA damage is extremely detrimental to cells. Theoretically, as genetic alterations do not arise at very low doses, the risk of carcinogenesis (and also several degenerative chronic diseases) is unlikely to occur after exposure to concentrations below the LOEL, as no biologically significant effects were observed experimentally. This outcome has implications on the numerous uses of pro-oxidant chemicals, including the uses as cosmetic bleaches, as cancer treatment agents, and in food production. Furthermore, this study strengthens the evidence of the existence of thresholds for direct-acting genotoxins.

#### SUPPLEMENTARY DATA

Supplementary data are available online at <http://toxsci.oxfordjournals.org/>.

#### FUNDING

Unilever.

#### ACKNOWLEDGMENTS

Certain commercial equipment, instruments, and materials are identified in this article to specify an experimental procedure as completely as possible. The identification of particular equipment or materials does not imply a recommendation or endorsement by the National Institute of Standards and Technology nor does it imply that the materials, instruments, or equipment are necessarily the best available for the purpose.

#### REFERENCES

- Ballmaier, D., and Epe, B. (1995). Oxidative DNA damage induced by potassium bromate under cell-free conditions and in mammalian cells. *Carcinogenesis* **16**, 335–342.
- Ballmaier, D., and Epe, B. (2006). DNA damage by bromate: Mechanism and consequences. *Toxicology* **221**, 166–171.
- Basu, A. K., Loechler, E. L., Leadon, S. A., and Essigmann, J. M. (1989). Genetic effects of thymine glycol: Site-specific mutagenesis and molecular modeling studies. *Proc. Natl. Acad. Sci. U.S.A.* **86**, 7677–7681.

- Boiteux, S., and Radicella, J. P. (2000). The human OGG1 gene: Structure, functions, and its implication in the process of carcinogenesis. *Arch. Biochem. Biophys.* **377**, 1–8.
- Cadet, J., Douki, T., and Ravanat, J. L. (2010). Oxidatively generated base damage to cellular DNA. *Free Radic. Biol. Med.* **49**, 9–21.
- Chung, S. H., Chung, S. M., Lee, J. Y., Kim, S. R., Park, K. S., and Chung, J. H. (1999). The biological significance of non-enzymatic reaction of menadione with plasma thiols: Enhancement of menadione-induced cytotoxicity to platelets by the presence of blood plasma. *FEBS Lett.* **449**, 235–240.
- Dhenaut, A., Boiteux, S., and Radicella, J. P. (2000). Characterization of the hOGG1 promoter and its expression during the cell cycle. *Mutat. Res.* **461**, 109–118.
- Dizdaroglu, M. (1985). Application of capillary gas chromatography-mass spectrometry to chemical characterization of radiation-induced base damage of DNA: Implications for assessing DNA repair processes. *Anal. Biochem.* **144**, 593–603.
- Doak, S. H., Brusehafer, K., Dudley, E., Quick, E., Johnson, G., Newton, R. P., and Jenkins, G. J. (2008). No-observed effect levels are associated with up-regulation of MGMT following MMS exposure. *Mutat. Res.* **648**, 9–14.
- Doak, S. H., Jenkins, G. J., Johnson, G. E., Quick, E., Parry, E. M., and Parry, J. M. (2007). Mechanistic influences for mutation induction curves after exposure to DNA-reactive carcinogens. *Cancer Res.* **67**, 3904–3911.
- Elhajouji, A., Lukamowicz, M., Cammerer, Z., and Kirsch-Volders, M. (2011). Potential thresholds for genotoxic effects by micronucleus scoring. *Mutagenesis* **26**, 199–204.
- Evans, M. D., Dizdaroglu, M., and Cooke, M. S. (2004). Oxidative DNA damage and disease: Induction, repair and significance. *Mutat. Res.* **567**, 1–61.
- Fenech, M. (2007). Cytokinesis-block micronucleus cytome assay. *Nat. Protoc.* **2**, 1084–1104.
- Forman, H. J., Zhang, H., and Rinna, A. (2009). Glutathione: Overview of its protective roles, measurement, and biosynthesis. *Mol. Aspects Med.* **30**, 1–12.
- Great Britain. Committee on Mutagenicity of Chemicals in Food. (2000). Guidance on a strategy for testing of chemicals for mutagenicity, Committee on Mutagenicity of Chemicals in Food, Consumer Products and the Environment.
- Guest, R. D., and Parry, J. M. (1999). P53 integrity in the genetically engineered mammalian cell lines AHH-1 and MCL-5. *Mutat. Res.* **423**, 39–46.
- Hartman, A. R., and Ford, J. M. (2003). BRCA1 and p53: Compensatory roles in DNA repair. *J. Mol. Med.* **81**, 700–707.
- Hatt, L., Loft, S., Risom, L., Moller, P., Sorensen, M., Raaschou-Nielsen, O., Overvad, K., Tjonneland, A., and Vogel, U. (2008). OGG1 expression and OGG1 Ser326Cys polymorphism and risk of lung cancer in a prospective study. *Mutat. Res.* **639**, 45–54.
- Henderson, L., Albertini, S., and Aardema, M. (2000). Thresholds in genotoxicity responses. *Mutat. Res.* **464**, 123–128.
- Jaruga, P., Kirkali, G., and Dizdaroglu, M. (2008). Measurement of formamidopyrimidines in DNA. *Free Radic. Biol. Med.* **45**, 1601–1609.
- Jenkins, G. J., Doak, S. H., Johnson, G. E., Quick, E., Waters, E. M., and Parry, J. M. (2005). Do dose response thresholds exist for genotoxic alkylating agents? *Mutagenesis* **20**, 389–398.
- Jeong, M. S., Lee, C. M., Jeong, W. J., Kim, S. J., and Lee, K. Y. (2010). Significant damage of the skin and hair following hair bleaching. *J. Dermatol.* **37**, 882–887.
- Kawanishi, S., and Murata, M. (2006). Mechanism of DNA damage induced by bromate differs from general types of oxidative stress. *Toxicology* **221**, 172–178.
- Loft, S., Høgh Danielsen, P., Mikkelsen, L., Risom, L., Forchhammer, L., and Møller, P. (2008). Biomarkers of oxidative damage to DNA and repair. *Biochem. Soc. Trans.* **36**, 1071–1076.
- Lutz, W. K., and Lutz, R. W. (2009). Statistical model to estimate a threshold dose and its confidence limits for the analysis of sublinear dose-response relationships, exemplified for mutagenicity data. *Mutat. Res.* **678**, 118–122.
- Mistry, P., and Herbert, K. E. (2003). Modulation of hOGG1 DNA repair enzyme in human cultured cells in response to pro-oxidant and antioxidant challenge. *Free Radic. Biol. Med.* **35**, 397–405.
- Naik, S., Tredwin, C. J., and Scully, C. (2006). Hydrogen peroxide tooth-whitening (bleaching): Review of safety in relation to possible carcinogenesis. *Oral Oncol.* **42**, 668–674.
- Nishimura, S. (2002). Involvement of mammalian OGG1(MMH) in excision of the 8-hydroxyguanine residue in DNA. *Free Radic. Biol. Med.* **32**, 813–821.
- Nutter, L. M., Ngo, E. O., Fisher, G. R., and Gutierrez, P. L. (1992). DNA strand scission and free radical production in menadione-treated cells. Correlation with cytotoxicity and role of NADPH quinone acceptor oxidoreductase. *J. Biol. Chem.* **267**, 2474–2479.
- Platel, A., Nesslany, F., Gervais, V., and Marzin, D. (2009). Study of oxidative DNA damage in TK6 human lymphoblastoid cells by use of the in vitro micronucleus test: Determination of no-observed-effect levels. *Mutat. Res.* **678**, 30–37.
- Powell, C. L., Swenberg, J. A., and Rusyn, I. (2005). Expression of base excision DNA repair genes as a biomarker of oxidative DNA damage. *Cancer Lett.* **229**, 1–11.
- Pryor, W. A. (1986). Oxy-radicals and related species: Their formation, lifetimes, and reactions. *Annu. Rev. Physiol.* **48**, 657–667.
- Saitoh, T., Shinmura, K., Yamaguchi, S., Tani, M., Seki, S., Murakami, H., Nojima, Y., and Yokota, J. (2001). Enhancement of OGG1 protein AP lyase activity by increase of APEX protein. *Mutat. Res.* **486**, 31–40.
- Sedelnikova, O. A., Redon, C. E., Dickey, J. S., Nakamura, A. J., Georgakilas, A. G., and Bonner, W. M. (2010). Role of oxidatively induced DNA lesions in human pathogenesis. *Mutat. Res.* **704**, 152–159.
- Smirnov, D. A., and Cheung, V. G. (2008). ATM gene mutations result in both recessive and dominant expression phenotypes of genes and microRNAs. *Am. J. Hum. Genet.* **83**, 243–253.
- Wallace, S. S. (2002). Biological consequences of free radical-damaged DNA bases. *Free Radic. Biol. Med.* **33**, 1–14.
- Zair, Z. M., Jenkins, G. J., Doak, S. H., Singh, R., Brown, K., and Johnson, G. E. (2011). N-methylpurine DNA glycosylase plays a pivotal role in the threshold response of ethyl methanesulfonate-induced chromosome damage. *Toxicol. Sci.* **119**, 346–358.